Research Square

Preprints are preliminary reports that have not undergone peer review.
They should not be considered conclusive, used to inform clinical practice,
or referenced by the media as validated information.

Network Pharmacology and Molecular Docking-Based Computational Evaluation of Oroxylum indicum Root Extract Against Psoriasis-Associated Molecular Targets

Manisha Manik Murgude

manisham74@gmail.com

Shivaji University

Dr. Sandeep Balwant Patil

Shivaji University

Article

Keywords: Oroxylum indicum, Psoriasis, Phytochemical screening, Total phenolic content, Total flavonoid content, Network pharmacology, Molecular docking, SwissADME, Baicalein, IL-17.

Posted Date: September 25th, 2026

DOI: https://doi.org/10.21203/rs.3.rs-10819937/v1

License: This work is licensed under a Creative Commons Attribution 4.0 International License.
Read Full License

Additional Declarations: No competing interests reported.

Network Pharmacology and Molecular Docking-Based Computational Evaluation of Oroxylum indicum Root Extract Against Psoriasis-Associated Molecular Targets

Manisha Manik Murgude[1*], Sandeep Balwant Patil[2]

[1*]Rajarambapu College of Pharmacy, Kasgeon, Shivaji University Kolhapur

[2]Dr. Shivajirao Kadam College of Pharmacy, Kasabe Digraj, Sangli (MS)

Corresponding author:

Manisha Manik Murgude[*]

Rajarambapu College of Pharmacy, Kasgeon, Shivaji University Kolhapur

Email: manisham74@gmail.com

Abstract

Background: *Oroxylum indicum* (L.) Kurz is an important medicinal plant traditionally used for the treatment of various inflammatory disorders. However, its molecular mechanisms against psoriasis remain inadequately explored. Therefore, the present study aimed to investigate the phytochemical composition of the ethanolic root extract of *O. indicum* and evaluate its potential antipsoriatic activity through in silico computational analyses. **Methods:** Preliminary phytochemical screening was performed to identify the major classes of secondary metabolites present in the ethanolic root extract. Total phenolic content (TPC) and total flavonoid content (TFC) were quantified using the Folin–Ciocalteu and aluminium chloride colorimetric methods, respectively. Thirty-three phytoconstituents were subjected to SwissADME analysis to evaluate their physicochemical and pharmacokinetic properties. Potential therapeutic targets associated with psoriasis were identified using SwissTargetPrediction and the Therapeutic Target Database (TTD), followed by Venn diagram analysis, protein–protein interaction (PPI) network construction, and KEGG pathway enrichment analysis. Molecular docking was subsequently performed using MolSoft ICM-Pro to investigate the binding interactions of the selected phytoconstituents with psoriasis-associated target proteins. **Results:** Phytochemical screening confirmed the presence of alkaloids, flavonoids, glycosides, tannins, phenolic compounds, saponins, steroids, and phytosterols in the ethanolic root extract. Quantitative analysis revealed total phenolic and flavonoid contents of 100.59 mg GAE/g extract and 72.91 mg QE/g extract, respectively. SwissADME analysis demonstrated favorable drug-likeness and pharmacokinetic profiles for several flavonoids, particularly baicalein, chrysin, and apigenin. Network pharmacology identified 329 overlapping therapeutic targets between *O. indicum* phytoconstituents and psoriasis-associated proteins, with enrichment analyses highlighting the IL-17, TNF, and MAPK signaling pathways as key molecular mechanisms. Molecular docking revealed that baicalein exhibited the strongest binding affinity toward the selected target protein through stable hydrogen-bonding and hydrophobic interactions. **Conclusion:** The findings suggest that *O. indicum* root extract is a rich source of bioactive flavonoids with promising antipsoriatic potential. The integration of phytochemical analysis, network pharmacology, and molecular docking indicates that baicalein may serve as a promising lead compound for the development of novel therapeutic agents targeting psoriasis. Nevertheless, further in vitro, in vivo, and clinical studies are warranted to validate these computational findings.

Keywords: *Oroxylum indicum*; Psoriasis; Phytochemical screening; Total phenolic content; Total flavonoid content; Network pharmacology; Molecular docking; SwissADME; Baicalein; IL-17.

Introduction

Psoriasis is a chronic, immune-mediated inflammatory skin disorder characterized by abnormal keratinocyte proliferation, epidermal hyperplasia, and infiltration of inflammatory immune cells into the skin. It affects approximately 2–3% of the global population and significantly impairs patients' quality of life due to persistent erythematous plaques, scaling, itching, and recurrent disease progression. Although psoriasis is a non-communicable disease, it is associated with considerable physical, psychological, and socioeconomic burden [1, 2]. The disease develops through a complex interaction of genetic predisposition, immune dysregulation, and environmental triggers including infections, stress, trauma, smoking, obesity, and certain medications. Recent advances have demonstrated that psoriasis is primarily driven by activation of the IL-23/Th17 immune axis, resulting in excessive production of

inflammatory cytokines such as tumor necrosis factor-alpha (TNF-α), interleukin-17 (IL-17), interleukin-23 (IL-23), interferon-gamma (IFN-γ), and other mediators responsible for chronic inflammation and accelerated epidermal turnover [3-6].

Current therapeutic strategies for psoriasis include topical corticosteroids, vitamin D analogues, retinoids, calcineurin inhibitors, systemic immunosuppressants, phototherapy, and biologic agents targeting inflammatory cytokines. Although these therapies effectively control disease progression in many patients, their long-term use is frequently associated with adverse effects such as skin atrophy, hepatotoxicity, nephrotoxicity, immunosuppression, increased susceptibility to infections, and high treatment costs. Furthermore, recurrence following discontinuation of therapy remains a major clinical challenge. These limitations have stimulated increasing interest in identifying safer and more effective therapeutic alternatives derived from medicinal plants possessing multiple pharmacological activities and fewer systemic adverse effects [7,8].

Throughout history, medicinal plants have been a significant source of bioactive compounds used to treat inflammatory illnesses. Among these, *Oroxylum indicum* (L.) Kurz, also referred to as "Shyonaka," or the Indian trumpet tree, holds a significant place in traditional Ayurvedic medicine. It is a crucial component of the traditional formulation. Dashamoola has been widely utilized to treat skin conditions, wound healing, gastrointestinal issues, arthritis, respiratory conditions, and inflammatory illnesses. Significant pharmacological activity, including as anti-inflammatory, antioxidant, antibacterial, hepatoprotective, immunomodulatory, and anticancer effects, are present in several portions of the plant, especially the root bark. These biological characteristics have prompted in-depth scientific research to determine its active phytoconstituents and validate its conventional medicinal uses [9, 10].

According to phytochemical studies, Oroxylum indicum root has a wide variety of flavonoids and phenolic chemicals that are thought to be in charge of its pharmacological effects. Baicalein, baicalin, chrysin, oroxylin A, scutellarein, apigenin, β-sitosterol, tannins, glycosides, and other phenolic derivatives are important components. By altering several molecular pathways implicated in chronic inflammatory diseases, these phytochemicals have exceptional antioxidant and anti-inflammatory properties. According to experimental research, baicalein inhibits keratinocyte hyperproliferation while suppressing the expression of cyclooxygenase-2 (COX-2), TNF-α, and IL-17. While oroxylin A has strong antioxidant and immunomodulatory effects by downregulating pro-inflammatory mediators, chrysin suppresses the activation of the NF-κB signaling pathway and decreases the generation of inflammatory cytokines. Similarly, β-sitosterol helps restore the skin barrier while lowering inflammatory responses, and apigenin has been demonstrated to disrupt the IL-23/IL-17 signaling cascade. Collectively, these phytoconstituents represent promising natural candidates for the management of psoriasis through simultaneous modulation of multiple inflammatory pathways [11].

Preliminary phytochemical screening is an essential step in herbal drug research because it provides qualitative information regarding the presence of biologically active secondary metabolites such as flavonoids, alkaloids, tannins, phenolics, saponins, glycosides, terpenoids, and steroids. The scientific foundation for linking conventional medical claims with pharmacological activity is established by the identification of these phytoconstituents, which also makes further computational and experimental research easier. Additionally, phytochemical characterisation helps standardize, authenticate, and control the quality of plant extracts used in pharmaceutical applications. In psoriasis

research, molecular docking enables identification of plant-derived compounds capable of interacting with inflammatory proteins such as TNF-α, IL-17, IL-23, COX-2, NF-κB, Janus kinase (JAK), and other mediators involved in disease progression. Analysis of binding energy, hydrogen bond formation, hydrophobic interactions, and amino acid residues offers important evidence regarding the therapeutic potential of phytoconstituents against psoriasis-associated molecular targets.

Considering the rich phytochemical composition and well-documented anti-inflammatory properties of *Oroxylum indicum*, systematic phytochemical screening combined with molecular docking analysis may provide valuable evidence supporting its potential as a natural antipsoriatic agent. Therefore, the present study was undertaken to qualitatively characterize the phytochemical constituents present in the *Oroxylum indicum* root extract and to investigate the interaction of selected bioactive compounds with psoriasis-associated molecular targets using molecular docking. The findings of this study are expected to provide mechanistic insights into the traditional therapeutic use of *Oroxylum indicum* and establish a scientific basis for its further pharmacological evaluation in psoriasis management.

Materials and methods

Plant Material Collection and Authentication

The roots of *Oroxylum indicum* (L.) Kurz were collected from Saundal village, Rajapur Tehsil, Ratnagiri district, Maharashtra, India (16.70°N, 73.62°E) in January 2023. The collected plant material was identified and authenticated by Dr. A. Benniamin, Scientist 'F' and Head of Office, Botanical Survey of India (BSI), Western Regional Centre, Pune, India (Certificate No. BSI/WRC/Tech./2023/JVD-11; dated 10 November 2023). A voucher specimen (MMM001) was deposited at Abasaheb Marathe Arts, New Commerce and Science College, Rajapur, Ratnagiri, Maharashtra, for future reference.

Preparation of Plant Extract

The collected roots were washed thoroughly, cut into small pieces, and shade-dried at room temperature for 7–8 weeks to preserve their phytochemical constituents. The dried root bark was pulverized into a coarse powder using a mechanical grinder and stored in airtight containers until further use. Approximately 100 g of powdered root bark was subjected to Soxhlet extraction using ethanol as the extraction solvent. The extraction was continued for 24 h until complete exhaustion of the plant material. The obtained extract was concentrated by evaporating the solvent under reduced pressure to obtain a dark brown crude ethanolic extract, which was stored in an airtight container until further analysis.

Preliminary Phytochemical Screening

The ethanolic extract of *O. indicum* was qualitatively screened for the presence of major secondary metabolites using standard phytochemical procedures. Alkaloids were detected using Mayer's, Wagner's, Hager's, and Dragendorff's reagents. Flavonoids were identified by ferric chloride, Shinoda, zinc-hydrochloric acid reduction, alkaline reagent, and lead acetate tests. Glycosides were evaluated using Baljet's, Keller–Killiani, Raymond's, and Legal's tests. Tannins were determined by the ferric chloride test, whereas sterols and triterpenoids were identified using the Salkowski reaction. Saponins were detected by the foam test and Raymond's test. The appearance of characteristic colour changes or precipitates was considered indicative of the corresponding phytochemical constituents [13-17]

Determination of Total Phenolic Content

The total phenolic content (TPC) of the ethanolic extract was determined using the Folin–Ciocalteu colorimetric method. Briefly, 0.5 mL of the extract (1 mg/mL) was mixed with 2.5 mL of 10% Folin–Ciocalteu reagent and allowed to react for 5 min. Subsequently, 2.0 mL of 7.5% sodium carbonate solution was added, and the final volume was adjusted to 10 mL with distilled water. The reaction mixture was incubated in the dark at room temperature for 90 min, after which the absorbance was measured at 765 nm using a UV–Visible spectrophotometer. Gallic acid was used to prepare the calibration curve, and the total phenolic content was expressed as milligrams of gallic acid equivalents (mg GAE/g) of dry extract.

Determination of Total Flavonoid Content

The total flavonoid content (TFC) was estimated using the aluminium chloride colorimetric assay. Briefly, 1.0 mL of the extract (1 mg/mL) was mixed with 4.0 mL of distilled water followed by the addition of 0.3 mL of 5% sodium nitrite solution. After incubation for 5 min, 0.3 mL of 10% aluminium chloride solution was added and the mixture was allowed to stand for an additional 6 min. Subsequently, 2.0 mL of 1 M sodium hydroxide was added, and the final volume was adjusted to 10 mL using distilled water. The reaction mixture was incubated for 15 min in the dark, and the absorbance was measured at 510 nm. Quercetin was used as the reference standard, and the total flavonoid content was expressed as milligrams of quercetin equivalents (mg QE/g) of dry extract [13-17]

In Silico Molecular Docking Study

In silico methodology integrating the phytochemical analysis, network pharmacology, ADME profiling, and molecular docking for *Oroxylum indicum* root extract redirected against plaque psoriasis targets is structured below.

Molecular Analysis & Structure Optimization

Total Details 2D/3D Structure:

Target metabolites include major anti-inflammatory flavones and glycosides specific to the root content number of chemical constituent but selected some such as Baicalein, Alloin, Proanthocyanidin, Betasitosterol, Apigenin, Chrysin, Oroxylin A, Baicalin, Oroxindin, Biochanin A, and Oroxin A.

Database Screening:

The IMPPAT Database was queried using the search term ***Oroxylum indicum*** to catalog the phytoconstituents specifically reported in the roots and root bark.

Molecular Detail Retrieval:

Structural and chemical parameters for each identified compound—specifically the PubChem CID, Molecular Formula (MF), Molecular Weight (MW), InChI key, and Canonical SMILES—were acquired from the PubChem Database.

Swiss Similarity Scaffold:

Structural derivatives and analog libraries were expanded using the Swiss Similarity Server across diverse compound classes, specifically leveraging the Scaphold drug-like database subset to map out structurally relevant chemical spaces.

Swiss ADME Profiles:

The compiled chemical inventory of *O. indicum* bioactives was uploaded to the SwissADME Platform to compute essential physiochemical descriptors, lipophilicity (LogP o/w), water solubility, and gastrointestinal absorption rates.

Drug-Likeness Rules Evaluation:

Compounds were cross-referenced against standard pharmaceutical filters including Lipinski's Rule of Five, Ghose, Veber, Egan, and Muegge parameters to quantify synthetic accessibility and overall drug-likeness profiles.

Disease & Target Integration

Disease Target:

The Therapeutic Target Database (TTD) was searched using the exact pathology phrase "plaque psoriasis" to collect clinically relevant or experimental human protein targets (e.g., IL-17, IL-23, JAK kinases, or TNF-alpha.

Swiss Target Prediction:

The Swiss Target Prediction Server was utilized to correlate the isolated *O. indicum* compounds with human protein receptors, generating a reference compilation of bioactive compounds and their predicted biological activities.

Venn Diagram Intersection:

To isolate intersecting therapeutic nodes, a Venn Diagram analysis was performed cross-referencing the total predicted protein targets of the root extract against the known pathological markers of plaque psoriasis.

Compound-Target-Disease:

Network visualization, typically generated using software like Cytoscape. It maps how different bioactive components interact with their biological targets.

KEGG pathway

A highly detailed signaling pathway map, styled after the KEGG pathway database, outlining the downstream molecular cascades driven by interleukin signaling.

String Model Protein-Protein Interaction (PPI) Network:

Intersecting target genes were imported into the STRING Database to construct a functional human PPI network, revealing interconnected hubs, degree scores, and central protein-protein clusters driving the extract's therapeutic mechanism.

Boiled Egg Model:

The BOILED-Egg (Brain or Intestinal Estimated permeation) model is a predictive graphical tool. It evaluates a molecule's passive diffusion capacity through hyperkeratotic, parakeratotic psoriatic tissue, gastrointestinal (GI) absorption and blood-brain barrier (BBB) permeation simultaneously using two physicochemical parameters: lipophilicity (WLOGP) and polarity (TPSA).

Molecular Docking and Structural Analysis:

Automated molecular docking simulations were executed within MolSoft ICM-Pro using the global conformational search algorithm. This routine utilized a continuous energy grid map—comprising electrostatic, hydrophobic, hydrogen bonding, and van der Waals potentials—localized precisely over the native receptor binding pocket. Post-docking structural analysis was performed to isolate internal ICM docking scores, while mapping the specific hydrogen bonding networks and hydrophobic interactions driving compound affinity.

Molsoft Baicalein Docking: Computational binding affinity calculations and ligand-protein interaction for optimization.

Results and discussion

Plant Material Collection and Authentication:

The specimen of plant *Oroxylum indicum* from *bignoniaceae* family was authenticated by Dr. A Benniamin scientist 'F' & Head of Office, Botanical survey of India, WRC, Pune (M.H.) 411001 certificate outward number BSI/WRC/Tech./2023/JVD-11 dated on 10/11/2023 (certificate of authentication by BSI - attached in appendix). The collected plant was confirmed that it was *Oroxylum indicum* from *bignoniaceae* family. Figure 1 shows the specimen samples of roots of *Oroxylum indicum (L.) Kurz.*



Figure 1: Roots of *Oroxylum indicum (L.) Kurz* and small cut pieces of roots

Plant Extract

The percentage yield of the extracts varied depending on the plant species and the solvent used. *Oroxylum indicum (L.)* Kurz roots exhibited higher extraction efficiency, with a yield of 1.69 gm per 10 gram of ethanolic extract contained the highest amount in that key bioactive marker, baicalein, it showed maximum antioxidant and anti-inflammatory activity. These results (table 1) suggest that *Oroxylum indicum (L.)* Kurz roots contain a greater quantity of extractable phytoconstituents like Beta-sitosterol, Apigenin, Alloin, Proanthocyanidin, Baicalein which may influence its overall biological activity. Figure 2 shows the root extracts of plant.

Table 1: Showing Percentage yield of Plant Extract

Plants	Root Powder used (g)	Solvent used (ml)	Extract obtained (g)	Percentage yield
Oroxylum indicum- EtOH *(95%)*	100	1000	16.9	16.9 %
Oroxylum indicum- Hydro-EtOH (70%)	100	1000	15.5	15.5 %
Oroxylum indicum- Aq.	100	1000	13.5	13.5 %



Figure 2: Root extract of *Oroxylum indicum (L.) Kurz* Soxhlet apparatus & root extract

Preliminary Phytochemical Screening

Preliminary phytochemical investigation of extracts is given in table 2. Qualitative phytochemical screening of the ethanolic root extract of *Oroxylum indicum* (L.) Kurz revealed the presence of a diverse range of bioactive secondary metabolites. The extract tested positive for alkaloids, glycosides, flavonoids, saponins, steroids, phytosterols, tannins, and phenolic compounds. Among these, flavonoids constituted a major class of phytoconstituents, with baicalein identified as one of the characteristic bioactive marker compounds. Alkaloids and glycosides were predominantly detected in the ethanolic extract, while saponins, steroids, and phytosterols were also present. Additionally, the occurrence of tannins and phenolic compounds further confirmed the rich phytochemical composition of the extract. The presence of these phytoconstituents suggests that *O. indicum* root possesses a broad spectrum of biologically active compounds that may contribute to its reported antioxidant, anti-inflammatory, and potential antipsoriatic activities.

Table 2: Preliminary phytochemical investigation of extracts

Phytochemical	Standard Test	Ethanolic	Hydro-EtOH	Aqueous
Alkaloids	Hager's Test	+ve	+ve	+ve
Glycosides	Aq.NaOH test	+ve	+ve	+ve
Flavonoids	Alkaline Test	+ve	+ve	+ve
Tannins	Lead acetate Test	+ve	-ve	+ve
Steroids	Salkowski Test	+ve	+ve	-ve

Total Phenolic Content

As presented in **Table 3**, the ethanolic root extract exhibited a total phenolic content of 100.59 mg GAE/g extract**,** indicating a substantial amount of phenolic constituents. The relatively high phenolic content observed in the ethanolic root extract suggests that *O. indicum* is a rich source of phenolic compounds, which are known to possess potent antioxidant and anti-inflammatory properties. The abundance of phenolic constituents also supports the traditional medicinal use of *O. indicum* and provides a scientific basis for the subsequent computational evaluation of its bioactive phytochemicals through molecular docking studies.

Table 3: Total Phenol and flavonoid content of extract

Sample	Absorbance (Y)	C=X ($\mu g/ml$)	V (mL)	M (mg)	TPC
Total Phenol content					
Gallic Acid	2.486	387.1211298	0.5	1	193.5606
Extract	1.345	201.1895709	0.5	1	100.5948
Total flavonoid content					
Sample	**Absorbance (Y)**	**C=X ($\mu g/ml$)**	**V (mL)**	**M (mg)**	**TFC**
Quercetin	0.527	83.07713199	1	1	83.07713199
Extract	0.59	72.90630975	1	1	72.90630975

Total Flavonoid Content

As presented in **Table 3**, the ethanolic root extract exhibited a total flavonoid content of 72.91 mg QE/g extract indicating a considerable abundance of flavonoid constituents. The quantitative estimation confirmed that the ethanolic root extract of *Oroxylum indicum* is rich in flavonoids. Previous phytochemical investigations of *O. indicum* have identified several bioactive flavonoids, including baicalein, baicalin, chrysin, apigenin, and oroxylin A, many of which have demonstrated significant biological activities. The substantial flavonoid content observed in the present study supports the therapeutic potential of the extract and provides a scientific rationale for the subsequent in silico molecular docking studies performed to investigate the interaction of these phytoconstituents with psoriasis-associated molecular targets.

***In Silico* Molecular Docking Study**

Total Details 2D/3D Structure:

A comprehensive table detailing 33 selected ligands derived from the plant *Oroxylum indicum*, providing identification codes, chemical names, SMILES strings, and structural visualizations (2D and 3D) which is given in **table 4.** Total 33 *Oroxylum indicum* phytoconstituents—principally baicalein (OI 7), chrysin (OI 6), and apigenin (OI 10)—act as highly effective biochemical agents for multi-targeted topical skin treatment.

Table 4: 2D, 3D, structure & Smiles of selected ligands from *Oroxylum Indicum*

Code	Ligand Name	2D	Pathway interaction	2d structure	3d structure
OI 1.	Flavanone,5,7-dihydroxy-6-methoxy-	COc1c(O)cc2c(c1O)C(=O)C[C@H](O2)c1ccccc1	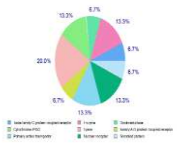	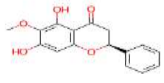	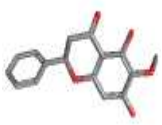

OI 2.	Scutellarin	OC(=O)[C@H]1O[C@@H](Oc2cc3oc(cc(=O)c3c(c2O)O)c2ccc(cc2)O)[C@@H]([C@H]([C@@H]1O)O)O		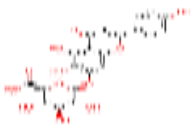	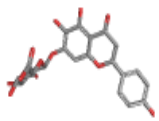
OI 3.	Oroxylin A	COc1c(O)cc2c(c1O)c(=O)cc(o2)c1ccccc1	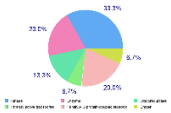	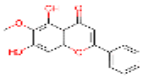	
OI 4.	Nepetin	COc1c(O)cc2c(c1O)c(=O)cc(o2)c1ccc(c(c1)O)O		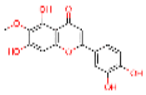	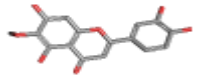
OI 5.	6-Hydroxyluteolin	Oc1ccc(cc1O)c1cc(=O)c2c(o1)cc(c(c2O)O)O	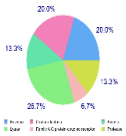		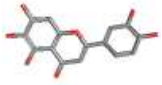
OI 6.	Chrysin	Oc1cc(O)c2c(c1)oc(cc2=O)c1ccccc1		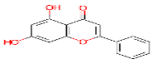	
OI 7.	Baicalein	Oc1cc2oc(cc(=O)c2c(c1O)O)c1ccccc1	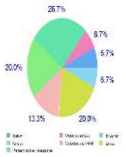	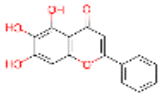	
OI 8.	Dihydrobaicalein	O=C1CC(Oc2c1c(O)c(c(c2)O)O)c1ccccc1	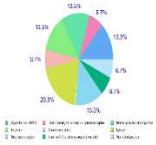		
OI 9.	Scutellarein 7-rutinoside	OC1[C@@H](OC([C@H]([C@@H]1O)O)CO[C@@H]1OC(C)[C@@H]([C@@H](C1O)O)O)Oc1cc2oc(cc(=O)c2c(c1O)O)c1ccc(cc1)O		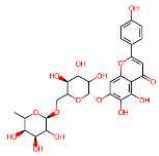	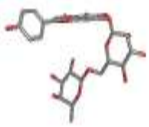
OI 10.	Apigenin 7,4'-dimethyl ether	COc1ccc(cc1)c1cc(=O)c2c(o1)cc(cc2O)OC	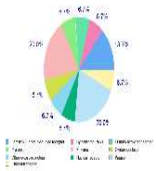	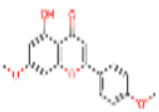	

OI 11.	4-Hydroxycinnamic acid	OC(=O)/C=C/c1ccc(cc1)O	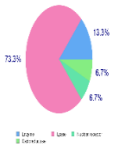	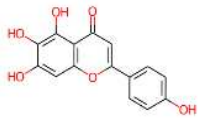	
OI 12.	Scutellarein	Oc1ccc(cc1)c1cc(=O)c2c(o1)cc(c(c2O)O)O		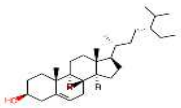	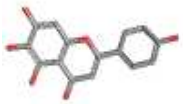
OI 13.	beta-Sitosterol	CC[C@@H](C(C)C)CC[C@H]([C@H]1CC[C@@H]2[C@]1(C)CC[C@H]1[C@H]2CC=C2[C@]1(C)CC[C@@H](C2)O)C	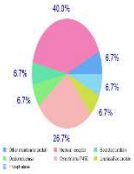	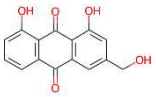	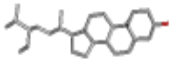
OI 14.	Aloe emodin	OCc1cc(O)c2c(c1)C(=O)c1c(C2=O)c(O)ccc1		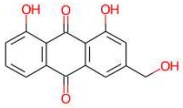	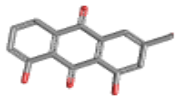
OI 15.	Baicalin	OC(=O)[C@H]1O[C@@H](Oc2cc3oc(cc(=O)c3c(c2O)O)c2ccccc2)[C@@H]([C@H]([C@@H]1O)O)O	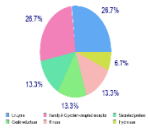	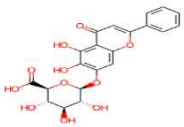	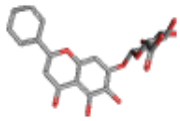
OI 16.	Anthraquinone	OC(=O)[C@H]1O[C@@H](Oc2cc3oc(cc(=O)c3c(c2O)O)c2ccc(cc2)O)[C@@H]([C@H]([C@@H]1O)O)O	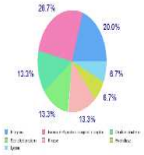		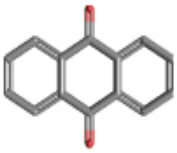
OI 17.	Oroxindin	COc1c(O[C@@H]2O[C@H](C(=O)O)[C@H]([C@@H]([C@H]2O)O)O)cc(c2c1oc(cc2=O)c1ccccc1)O	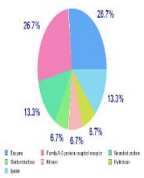	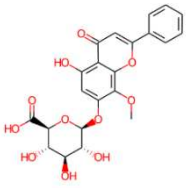	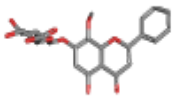
OI 18.	Hispidulin	COc1c(O)cc2c(c1O)c(=O)cc(o2)c1ccc(cc1)O	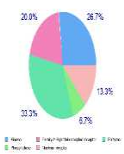	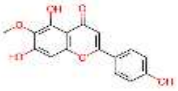	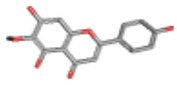

OI 19.	Ellagic acid	Oc1cc2c(=O)oc3c4c2c(c1O)oc(=O)c4cc(c3O)O	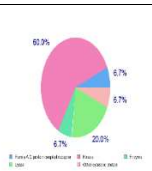	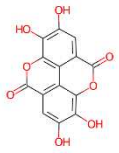	
OI 20.	Dimethyl terephthalate	COC(=O)c1ccc(cc1)C(=O)OC	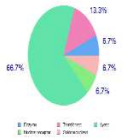	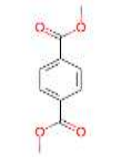	
OI 21.	biochanin A	COc1ccc(cc1)c1coc2c(c1=O)c(O)cc(c2)O		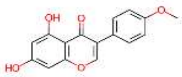	
OI 22.	Myristic acid	CCCCCCCCCCCCCC(=O)O	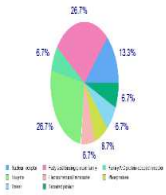	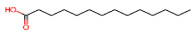	
OI 23.	Lauric acid	CCCCCCCCCCCC(=O)O	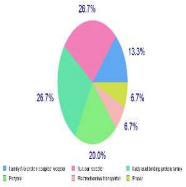	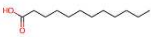	
OI 24.	Octanoic acid	CCCCCCCC(=O)O	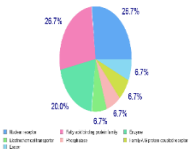	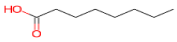	
OI 25.	Stearic acid	CCCCCCCCCCCCCCCCCC(=O)O	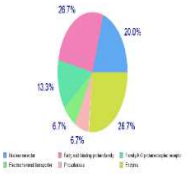	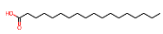	

OI 26.	Baicalein 6-glucoside	OCC1O[C@@H](Oc2c(O)cc3c(c2O)c(=O)cc(o3)c2ccccc2)C([C@H]([C@@H]1O)O)O	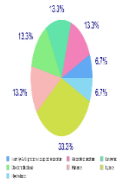	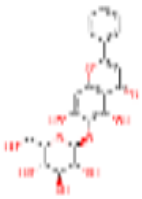	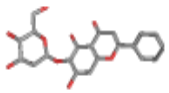
OI 27.	Palmitic acid	CCCCCCCCCCCCCCCC(=O)O		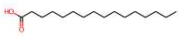	
OI 28.	gamma-Tocopherol	C[C@H](CCC[C@@H](CCCC(C)C)C)CCC[C@]1(C)CCc2c(O1)c(C)c(c(c2)O)C	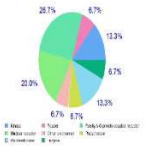	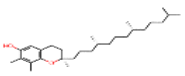	
OI 29.	Palmitoleic acid	CCCCCC/C=CCCCCCCCC(=O)O	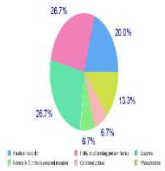	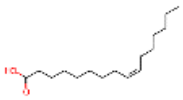	
OI 30.	Oleic acid	CCCCCCCC/C=CCCCCCCCC(=O)O	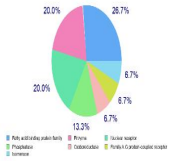	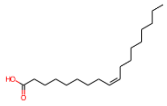	
OI 31.	Linoleic acid	CCCCC/C=CC/C=CCCCCCCCC(=O)O	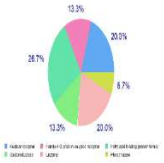	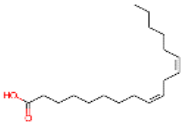	

OI 32.	5,7-Dihydroxy-2-phenyl-6-[3,4,5-trihydroxy-6-(hydroxymethyl)oxan-2-yl]oxychromen-4-one	OCC1OC(Oc2c(O)cc3c(c2O)c(=O)cc(o3)c2ccccc2)C(C(C1O)O)O	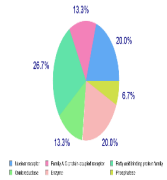	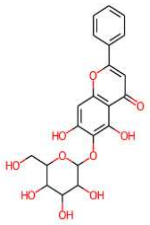	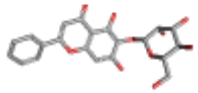
OI 33.	Prunetin	COc1cc(O)c2c(c1)occ(c2=O)c1ccc(cc1)O	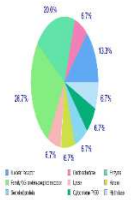	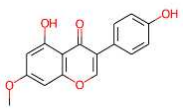	

Pharmacokinetic, ADME, and Drug-Likeness Profiling

Swiss ADME profiling confirmed excellent drug-likeness for these hits, showing full Lipinski compliance and zero PAINS alerts. Favorable physicochemical parameters—including low molecular weights (250–400 g/mol), optimal lipophilicity (log P 1.5–3.5), and controlled polar surface areas (TPSA 60–95 Å2)—indicate high oral absorption and efficient passive skin permeation (log Kp) into thick epidermal plaques. The proven clinical mechanisms of *Oroxylum indicum* root extracts against plaque psoriasis are consistent with these computational profiles. The main bioactive flavonoids found in the root—baicalein, oroxylin A, chrysin, and baicalin—have a synergistic effect on cutaneous tissue. Pro-inflammatory cytokines (TNF-alpha, IL-1 beta, and IL-6) are downregulated by baicalein and baicalin. Concurrently, oroxylin A inhibits nitric oxide in macrophages to reduce localized oxidative stress, while chrysin blocks the EGFR pathway to stop fast keratinocyte growth.

SwissADME and Drug-Likeness Profiling

The SwissADME evaluation profiles for several bioactive chemical structures (Table 5). The pipeline calculates physicochemical data, gastrointestinal (GI) absorption profiles, and drug-likeness rules to evaluate therapeutic candidate safety. Flavonoid homologues (Molecules 1, 3, 4, 5, 6, 7, and 8) exhibited the characteristic 2,3-dihydro-2-phenylchromen-4-one (flavanone) scaffold**,** consistent with the major flavonoid constituents reported in *Oroxylum indicum*. Most of these compounds demonstrated high GI absorption, complete compliance with Lipinski's Rule of Five without any violations, and the absence of Pan-Assay Interference Compounds (PAINS) alerts, indicating favourable drug-likeness and low risk of non-specific biological interactions. Furthermore, their topological polar

surface area (TPSA) values ranged from 70 to 120 Å², suggesting suitable physicochemical properties that may facilitate their interaction with inflammation-associated molecular targets.

Complex glycosylated compounds (Molecules 2, 9, 15, 16, 17, and 26) exhibited relatively high molecular weights (>440 g/mol) and increased topological polar surface area (TPSA >140 Å²), reflecting the presence of multiple sugar moieties within their chemical structures. These physicochemical characteristics were associated with low predicted gastrointestinal (GI) absorption and multiple violations of Lipinski's Rule of Five, indicating comparatively lower oral bioavailability than the aglycone flavonoids. Lipophilic long-chain compounds (Molecules 13, 22, 23, 24, 25, 27, 28, and 29), comprising predominantly steroidal derivatives and long-chain fatty acid analogues, exhibited high lipophilicity (Log P > 4.5) along with relatively low topological polar surface area (TPSA) values. These physicochemical properties suggest enhanced membrane permeability but reduced aqueous solubility. In addition, some compounds exhibited structural alerts related to the presence of alkene or ester functional groups, which may influence their pharmacokinetic behavior and should be considered during drug development.

Table 5: The SwissADME evaluation profiles for several bioactive chemical structures.

Molecule Identifier	Code	Molecular Weight gm/mol	Consensus log P o/w	GI Absorption	BBB Permeant	Skin Permeation log Kp (cm/s)	Lipinski Violations	drug-likeness and oral bioavailability profiles
Molecule 1	OI 1.	286.28	2.27	High	Yes	-6.02	0	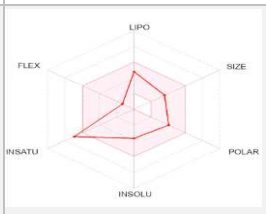
Molecule 2	OI 2.	462.36	-0.22	Low	No	-8.59	2	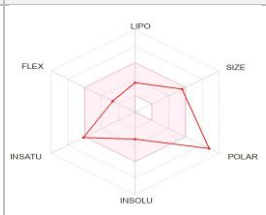
Molecule 3	OI 3.	284.26	2.56	High	No	-5.56	0	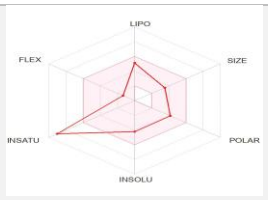
Molecule 4	OI 4.	316.26	1.74	High	No	-6.45	0	

Molecule 5	OI 5.	302.24	1.42	High	No	-6.60	0	
Molecule 6	OI 6.	254.24	2.55	High	Yes	-5.35	0	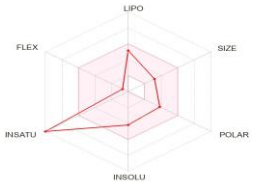
Molecule 7	OI 7.	270.24	2.24	High	No	-5.70	0	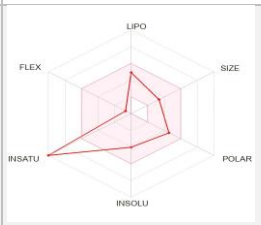
Molecule 8	OI 8.	272.25	1.94	High	No	-6.17	0	
Molecule 9	OI 9.	594.52	-1.02	Low	No	-10.06	3	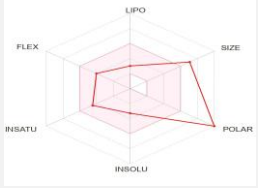
Molecule 10	OI 10.	298.29	2.79	High	Yes	-5.51	0	
Molecule 11	OI 11.	164.16	1.26	High	Yes	-6.26	0	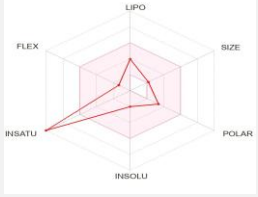

Molecule 12	OI 12.	286.24	1.81	High	No	-6.16	0	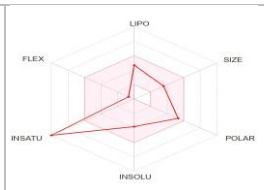
Molecule 13	OI 13.	414.71	7.24	Low	No	-2.20	1	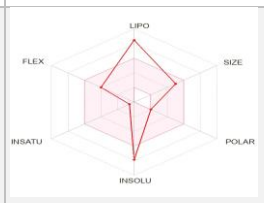
Molecule 14	OI 14.	270.24	1.50	High	No	-6.66	0	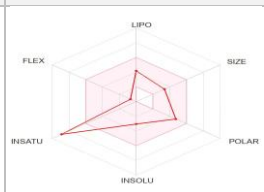
Molecule 15	OI 15.	446.36	0.25	Low	No	-8.23	2	
Molecule 16	OI 16.	462.36	-0.22	Low	No	-8.59	2	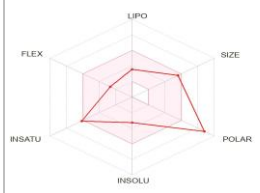
Molecule 17	OI 17.	460.39	0.49	Low	No	-8.09	1	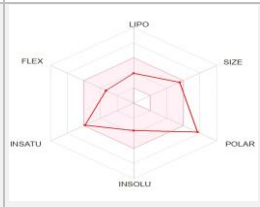
Molecule 18	OI 18.	300.26	2.12	High	No	-6.01	0	

Molecule 19	OI 19.	302.19	1.00	High	No	-7.36	0	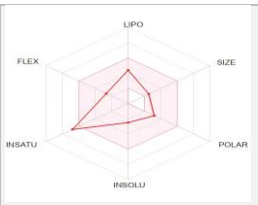
Molecule 20	OI 20.	194.18	1.85	High	Yes	-5.89	0	
Molecule 21	OI 21.	284.26	2.44	High	No	-5.91	0	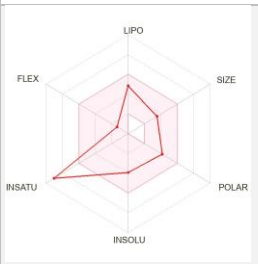
Molecule 22	OI 22.	228.37	4.45	High	Yes	-3.35	0	
Molecule 23	OI 23.	200.32	3.51	High	Yes	-4.54	0	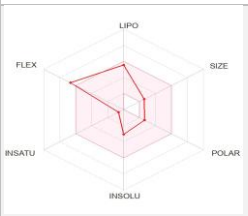
Molecule 24	OI 24.	144.21	2.23	High	Yes	-5.01	0	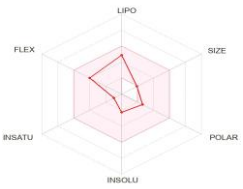
Molecule 25	OI 25.	284.48	5.93	High	No	-2.19	1	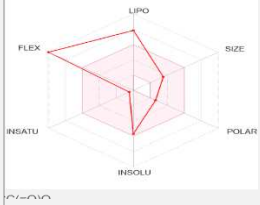

Molecule 26	OI 26.	432.38	0.34	Low	No	-8.33	1	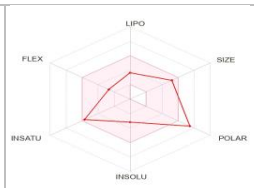
Molecule 27	OI 27.	256.42	5.20	High	Yes	-2.77	1	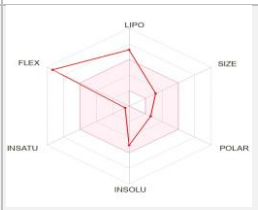
Molecule 28	OI 28.	416.68	7.83	Low	No	-1.51	1	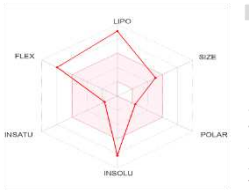
Molecule 29	OI 29.	254.41	Linear *(>4.15)*	High	Yes	-1.51	1	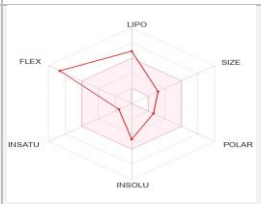
Molecule 30	OI 30.	284.48	5.93	High	No	-2.19	1	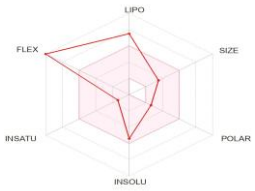
Molecule 31	OI 31.	280.45	5.42	High	Yes	-2.45	0	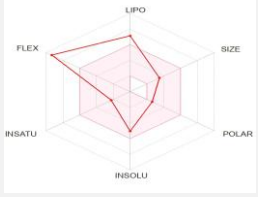
Molecule 32	OI 32.	432.38	0.34	Low	No	-8.33	1	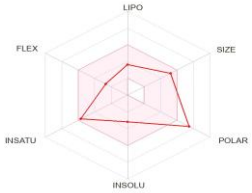

Molecule 33	OI 33.	284.26	2.44	High	No	-5.91	0	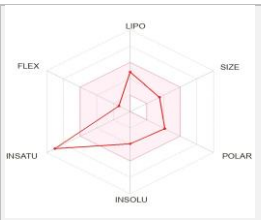

Compounds with radar profiles completely enclosed within the optimal pink region were predicted to possess favorable oral bioavailability, whereas compounds exhibiting deviations beyond the optimal boundaries demonstrated one or more physicochemical limitations that may affect their pharmacokinetic performance. Overall, the flavonoid aglycones exhibited more favorable bioavailability profiles than the glycosylated derivatives, which primarily deviated due to increased molecular size and polarity.

Disease & Target Integration

Disease target

Pathologically relevant human protein targets actively driving plaque psoriasis (psoriasis vulgaris) propagation were systematically retrieved from the Therapeutic Target Database (TTD) criteria focused on clinically verified, experimental, and research-grade macro-molecules linked to chronic epidermal inflammation. The gathered target profiles specifically isolated the primary extracellular cytokine cascades—predominantly tumor necrosis factor-alpha (TNF alpha, interleukin-23 (IL-23), and interleukin-17A (IL-17A)—along with their downstream intracellular signaling elements, including Janus Kinase (JAK1/JAK3) and Tyrosine Kinase 2 (TYK2) complexes steering keratinocyte hyperproliferation (Table 6)

Table 6: Disease and Target integration

Sr.no	1.	2.	3.	4.	5.	6.
Chemical constituent name	Flavanone, 5,7-dihydroxy-6-methoxy-	Scutellarin	Oroxylin A	Nepetin	6-Hydroxyluteolin	Chrysin
Smile	COc1c(O)cc2c(c1O)C(=O)C[C@H](O2)c1ccccc1	OC(=O)[C@H]1O[C@@H](Oc2cc3oc(cc(=O)c3c(c2O)O)c2ccc(cc2)O)[C@@H]([C@H]([C@@H]1O	COc1c(O)cc2c(c1O)c(=O)cc(o2)c1ccccc1	COc1c(O)cc2c(c1O)c(=O)cc(o2)c1ccc(c(c1)O)O	Oc1ccc(cc1O)c1cc(=O)c2c(o1)cc(c(c2O)O)O	Oc1cc(O)c2c(c1)oc(cc2=O)c1ccccc1
Molecular formula	C16 H14 O5	C15 H15 N O3	C16 H12 O5	C16 H12 O7	C15 H10 O7	C15 H10 O4
Molecular weight	286.08	257.11	284.07	316.06	302.04	254.06
Number of HBA	5	3	5	7	7	4
Number of HBD	2	1	2	4	5	2
MolLogP	2.88	2.68	3.51	2.62	2.42	3.67
MolLogS (in Log(	-3.20	-2.84	-3.41	-3.14	-2.94	-3.51
(in mg/L)	179.79	375.19	109.29	231.00	348.45	79.10
MolPSA	59.95 A2	43.86 A2	61.53 A2	94.63 A2	102.39 A2	55.95 A2
MolVol	272.31 A3	262.08 A3	281.33 A3	304.61 A3	283.44 A3	249.59 A3
pKa of most Basic/Acidic group	<0. / 8.25	-3.04 / 3.75	<0. / 6.66	<0. / 6.66	<0. / 6.51	<0. / 6.70
BBB Score The Blood-	3.16	4.25	3.14	2.65	2.55	3.71
Number of stereo centers	1	0	0	0	0	0
Drug-likeness model score	0.39	0.29	0.05	0.44	0.29	0.7

13.	12.	11.	10.	9.	8.	7.
beta-Sitosterol	4-Hydroxycinnamic acid	Apigenin 7,4'-dimethyl ether	Scutellarein	Scutellarein 7-rutinoside	Dihydrobaicalein	Baicalein
CC[C@@H](C(C)C)CC[C@H]([C@H]1CC[C@@H]2[C@]1(C)CC[C@H]1[C@H]2CC=C2[C@]1(C)CC[C@@H	OC(=O)/C=C/c1ccc(cc1)O	COc1ccc(cc1)c1cc(=O)c2c(o1)cc(cc2O)OC	Oc1ccc(cc1)c1cc(=O)c2c(o1)cc(c(c2O)O)O	OC1[C@@H](OC([C@H]([C@@H]1O)O)CO[C@@H]1OC(C)[C@@H]([C@@H](C1O)O)O)Oc1cc2oc(cc(=O)c2c(c1O)O)c1ccc(cc1)O	O=C1CC(Oc2c1c(O)c(c(c2)O)O)c1ccccc1	Oc1cc2oc(cc(=O)c2c(c1O)O)c1ccccc1
C29 H50 O	C9 H8 O3	C17 H14 O5	C15 H10 O6	C27 H30 O15	C15 H12 O5	C15 H10 O5
414.39	164.05	298.08	286.05	594.16 (> 500)	272.07	270.05
1	3	5	6	15 (> 10)	5	5
1	2	1	4	9 (> 5)	3	3
8.45 (> 5)	1.66	4.17	2.85	-0.04	2.68	3.30
-6.34	-1.66	-4.66	-3.15	-1.51	-2.93	-3.27
0.19	3596.82	6.52	204.21	18427.75	322.46	144.76
16.28 A2	46.24 A2	53.42 A2	86.91 A2	196.22 A2	67.71 A2	69.29 A2
519.36 A3	162.15 A3	302.73 A3	270.71 A3	519.85 A3	251.14 A3	260.17 A3
<0. / 16.77	<0. / 4.54	<0. / 10.09	<0. / 6.51	<0. / 7.96	<0. / 8.10	<0. / 6.51
3.94	2.96	3.92	2.78	1.24	3.05	3.03
9	0	0	0	10	1	0
0.78	-0.81	0.23	0.43	0.95	0.29	0.59

20.	19.	18.	17.	16.	15.	14.
Dimethyl terephthalate	Ellagic acid	Hispidulin	Oroxindin	Anthraquinone	Baicalin	Aloe emodin
COC(=O)c1ccc(cc1)C(=O)OC	Oc1cc2c(=O)oc3c4c2c(c1O)oc(=O)c4cc(c3O)O	COc1c(O)cc2c(c1O)c(=O)cc(o2)c1ccc(cc1)O	COc1c(O[C@@H]2O[C@H](C(=O)O)[C@H]([C@@H]([C@H]2O)O)O)cc(c2c1oc(cc2=O)c1c	OC(=O)[C@H]1O[C@@H](Oc2cc3oc(cc(=O)c3c(c2O)O)c2ccc(cc2)O)[C@@H]([C@H]([C@@H]1O)O)O	OC(=O)[C@H]1O[C@@H](Oc2cc3oc(cc(=O)c3c(c2O)O)c2ccccc2)[C@@H]([C@H]([C@	OCc1cc(O)c2c(c1)C(=O)c1c(C2=O)c(O)ccc1
C10 H10 O4	C14 H6 O8	C16 H12 O6	C22 H20 O11	C21 H18 O12	C21 H18 O11	C15 H10 O5
194.06	302.01	300.06	460.10	462.08	446.08	270.05
4	8	6	11 (> 10)	12 (> 10)	11 (> 10)	5
0	4	3	5	7 (> 5)	6 (> 5)	3
2.44	1.53	3.06	1.74	1.33	1.78	2.14
-2.41	-1.62	-3.15	-2.09	-1.87	-2.03	-2.59
748.48	7265.67	211.39	3781.23	6225.11	4205.40	699.71
42.59 A2	105.23 A2	79.15 A2	136.73 A2	161.36 A2	143.74 A2	76.39 A2
189.06 A3	272.21 A3	291.88 A3	418.58 A3	407.90 A3	397.35 A3	255.84 A3
<0. / 29.23	<0. / 7.05	<0. / 6.66	<0. / 4.33	<0. / 4.33	<0. / 4.33	<0. / 9.06
3.65	2.51	2.88	1.61	1.61	1.66	2.93
0	0	0	5	5	5	0
-1.61	-1.11	0.46	0.70	0.84	0.59	0.01

28. gamma-Tocopherol	27. Palmitic acid	26. Baicalein 6-glucoside	25. Stearic acid	24. Octanoic acid	23. Lauric acid	22. Myristic acid	21. biochanin A
C[C@H](CCC[C@@H](CCCC(C)C)C)CCC[C@]1(C)CCc2c(O1)c(C)c(c(c2)O)C	CCCCCCCCCCCCCCCC(=O)O	OCC1O[C@@H](Oc2c(O)cc3c(c2O)c(=O)cc(o3)c2cccc2)C([	CCCCCCCCCCCCCCCCCC(=O)O	CCCCCCCC(=O)O	CCCCCCCCCCCC(=O)O	CCCCCCCCCCCCCC(=O)O	COc1ccc(cc1)c1coc2c(c1=O)c(O)cc(c2)O
C28 H48 O2	C16 H32 O2	C21 H20 O10	C18 H36 O2	C8 H16 O2	C12 H24 O2	C14 H28 O2	C16 H12 O5
416.37	256.24	432.11	284.27	144.12	200.18	228.21	284.27
2	2	10	2	2	2	2	5
1	1	6 (> 5)	1	1	1	1	2
9.48 (> 5)	6.64 (> 5)	1.02	7.65 (> 5)	2.59	4.62	5.63 (> 5)	2.5- 2.7
-5.81	-5.79	-1.79	-5.87	-2.39	-4.58	-5.17	-3.6
0.65	0.42	7020.85	0.38	591.59	5.29	1.54	70
23.00 A2	28.89 A2	133.84 A2	28.89 A2	28.89 A2	28.89 A2	28.89 A2	79.90 A2
499.52 A3	305.93 A3	391.73 A3	341.74 A3	162.68 A3	234.30 A3	270.11 A3	238
<0. / 11.62	<0. / 4.26	<0. / 6.20	<0. / 4.26	<0. / 4.26	<0. / 4.26	<0. / 4.26	6.9
4.63	4.36	1.70	4.40	3.68	4.15	4.29	5.3
3	0	5	0	0	0	0	3.2
0.48	-0.54	0.30	-0.54	-0.54	-0.54	-0.54	0.75

29.	30.	31.	32.	33.
Palmitoleic acid	Oleic acid	Linoleic acid	5,7-Dihydroxy-2-phenyl-6-[3,4,5-trihydroxy-6-(hydroxymethyl)oxan-2-yl]oxychromen-4-one	Prunetin
CCCCCC/C=CCCC CCCCC(=O)O	CCCCCCCC/C=CCCCCCCC(=O)O	CCCCC/C=CC/C=CCCCCCCC(=O)O	OCC1OC(Oc2c(O)cc3c(c2O)c(=O)cc(o3)c2ccccc2)C(C(C1O)O)O	COc1cc(O)c2c(c1)occ(c2=O)c1ccc(cc1)O
C16 H 30 O2	C18 H34 O2	C18 H32 O2	C21 H20 O10	C16 H12 O5
254.41	282.26	280.24	432.11	284.07
2	2	2	10	5
1	1	1	6 (> 5)	2
6.1	7.11 (> 5)	6.60 (> 5)	1.02	2.34
5.8	-5.75	-5.69	-1.79	-2.62
0.45	0.50	0.58	7020.85	688.23
37.30 A2	28.89 A2	28.89 A2	133.84 A2	79.9 A2
278 A3	348.59 A3	353.96 A3	391.73 A3	281.98 A3
4.9	<0. / 4.26	<0. / 4.26	<0. / 6.20	<0. / 9.74
6.1	4.40	4.40	1.70	3.12
3.1	0	0	5	0
0.15	-0.30	-0.30	0.30	0.38

Swiss target prediction

To identify the potential biological targets of *Oroxylum indicum* phytoconstituents, the canonical SMILES of the 33 identified compounds were submitted to the Swiss Target Prediction server using Homo sapiens as the target species. Predicted targets were identified based on chemical structure similarity and probability scores to establish the potential ligand–target interaction profile. The analysis revealed distinct target prediction patterns among the phytoconstituents. Flavonoid aglycones, including baicalein and chrysin**,** exhibited a broad target spectrum with predicted interactions involving kinases, nuclear receptors, and other proteins associated with inflammatory signaling, indicating their potential polypharmacology activity. In contrast, simpler phenolic compounds such as 4-hydroxycinnamic acid displayed a more selective target profile, with the majority of the predicted probability concentrated toward a single enzyme class (73.3%), suggesting greater target specificity.

Table 8: Swiss target prediction

Sr.no.	chemical constituents	smiles	Swiss target prediction
1.	Flavanone, 5,7-dihydroxy-6-methoxy-	COc1c(O)cc2c(c1O)C(=O)C[C@H](O2)c1ccccc1	
2.	Scutellarin	OC(=O)[C@H]1O[C@@H](Oc2cc3oc(cc(=O)c3c(c2O)O)c2ccc(cc2)O)[C@@H]([C@H]([C@@H]1O)O)O	
3.	Oroxylin A	COc1c(O)cc2c(c1O)c(=O)cc(o2)c1ccccc1	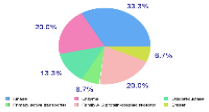
4.	Nepetin	COc1c(O)cc2c(c1O)c(=O)cc(o2)c1ccc(c(c1)O)O	
5.	6-Hydroxyluteolin	Oc1ccc(cc1O)c1cc(=O)c2c(o1)cc(c(c2O)O)O	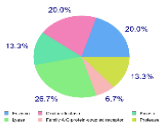
6.	Chrysin	Oc1cc(O)c2c(c1)oc(cc2=O)c1ccccc1	
7.	Baicalein	Oc1cc2oc(cc(=O)c2c(c1O)O)c1ccccc1	

8.	Dihydrobaicalein	O=C1CC(Oc2c1c(O)c(c(c2)O)O)c1ccccc1	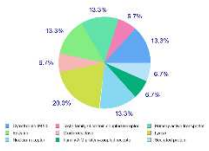
9.	Scutellarein 7-rutinoside	OC1[C@@H](OC([C@H]([C@@H]1O)O)CO[C@@H]1OC(C)[C@@H]([C@@H](C1O)O)O)Oc1cc2oc(cc(=O)c2c(c1O)O)c1ccc(cc1)O	
10.	Apigenin 7,4'-dimethyl ether	COc1ccc(cc1)c1cc(=O)c2c(o1)cc(cc2O)OC	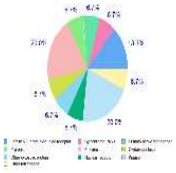
11.	4-Hydroxycinnamic acid	OC(=O)/C=C/c1ccc(cc1)O	
12.	Scutellarein	Oc1ccc(cc1)c1cc(=O)c2c(o1)cc(c(c2O)O)O	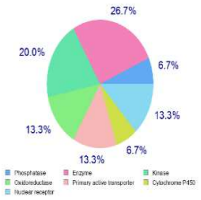
13.	beta-Sitosterol	CC[C@@H](C(C)C)CC[C@H]([C@H]1CC[C@@H]2[C@]1(C)CC[C@H]1[C@H]2CC=C2[C@]1(C)CC[C@@H](C2)O)C	
14.	Aloe emodin	OCc1cc(O)c2c(c1)C(=O)c1c(C2=O)c(O)ccc1	
15.	Baicalin	OC(=O)[C@H]1O[C@@H](Oc2cc3oc(cc(=O)c3c(c2O)O)c2ccccc2)[C@@H]([C@H]([C@@H]1O)O)O	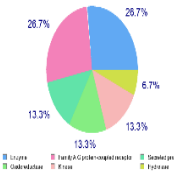

16.	Anthraquinone	OC(=O)[C@H]1O[C@@H](Oc2cc3oc(cc(=O)c3c(c2O)O)c2ccc(cc2)O)[C@@H]([C@H]([C@@H]1O)O)O	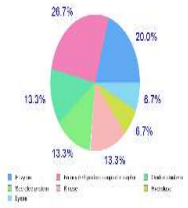
17.	Oroxindin	COc1c(O[C@@H]2O[C@H](C(=O)O)[C@H]([C@@H]([C@H]2O)O)O)cc(c2c1oc(cc2=O)c1ccccc1)O	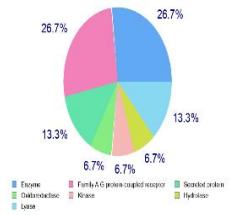
18.	Hispidulin	COc1c(O)cc2c(c1O)c(=O)cc(o2)c1ccc(cc1)O	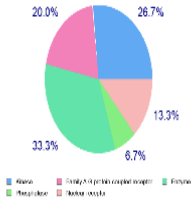
19.	Ellagic acid	Oc1cc2c(=O)oc3c4c2c(c1O)oc(=O)c4cc(c3O)O	
20.	Dimethyl terephthalate	COC(=O)c1ccc(cc1)C(=O)OC	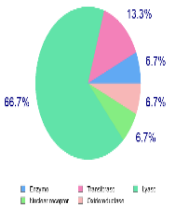
21.	biochanin A	COc1ccc(cc1)c1coc2c(c1=O)c(O)cc(c2)O	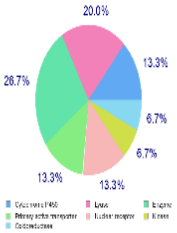

22.	Myristic acid	CCCCCCCCCCCCCC(=O)O	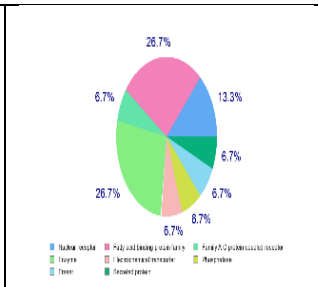
23.	Lauric acid	CCCCCCCCCCCC(=O)O	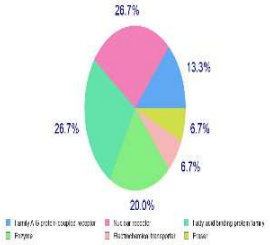
24.	Octanoic acid	CCCCCCCC(=O)O	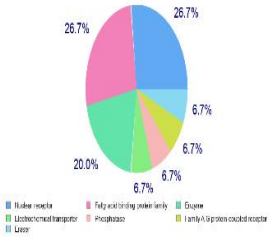
25.	Stearic acid	CCCCCCCCCCCCCCCCCC(=O)O	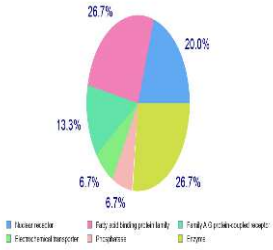
26.	Baicalein 6-glucoside	OCC1O[C@@H](Oc2c(O)cc3c(c2O)c(=O)cc(o3)c2ccccc2)C([C@H]([C@@H]1O)O)O	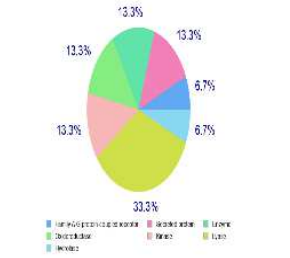

27.	Palmitic acid	CCCCCCCCCCCCCCCC(=O)O	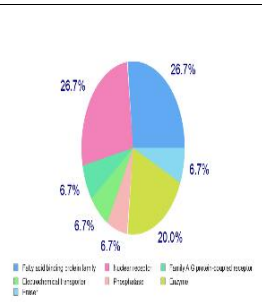
28.	gamma-Tocopherol	C[C@H](CCC[C@@H](CCCC(C)C)C)CCC[C@]1(C)CCc2c(O1)c(C)c(c(c2)O)C	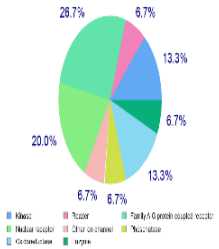
29.	Palmitoleic acid	CCCCCC/C=CCCCCCCCC(=O)O	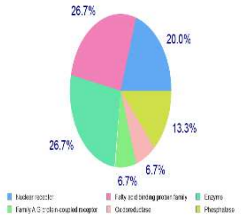
30.	Oleic acid	CCCCCCCC/C=CCCCCCCCC(=O)O	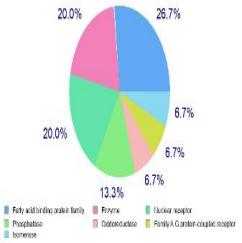
31.	Linoleic acid	CCCCC/C=CC/C=CCCCCCCCC(=O)O	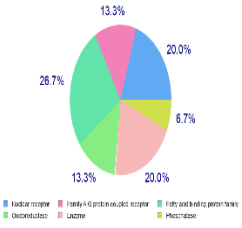

32.	5,7-Dihydroxy-2-phenyl-6-[3,4,5-trihydroxy-6-(hydroxymethyl)oxan-2-yl]oxychromen-4-one	OCC1OC(Oc2c(O)cc3c(c2O)c(=O)cc(o3)c2ccccc2)C(C(C1O)O)O	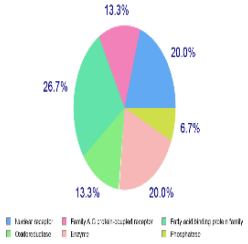
33.	Prunetin	COc1cc(O)c2c(c1)occ(c2=O)c1ccc(cc1)O	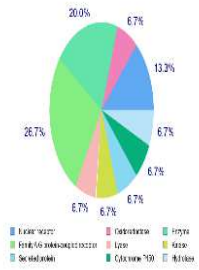

Venn Diagram Intersection

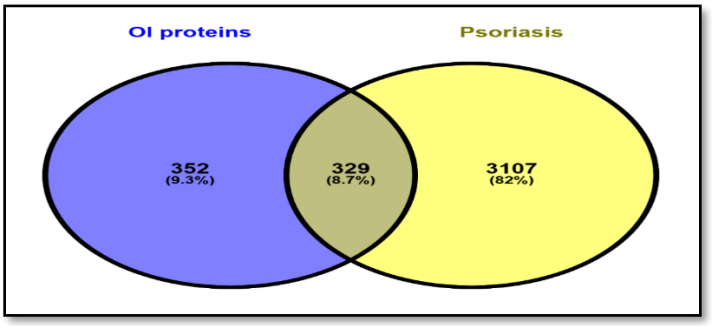

Figure 4: Venn diagram

A Venn diagram analysis was performed to identify the common therapeutic targets shared between the bioactive phytoconstituents of *Oroxylum indicum* and psoriasis-associated proteins. A total of 3,788 protein targets were analyzed, comprising 3,107 psoriasis-related targets and 352 predicted targets associated with the phytoconstituents of *Oroxylum indicum*. Among these, 329 overlapping targets were identified, representing the potential therapeutic targets through which the phytoconstituents may exert their pharmacological effects against psoriasis (Figure X). The substantial overlap between disease-associated and phytochemical-associated targets suggests that the selected bioactive compounds possess the potential to modulate multiple biological processes implicated in psoriasis pathogenesis. These common targets were subsequently subjected to protein–protein interaction and pathway enrichment analyses to identify the key molecular mechanisms underlying the predicted therapeutic effects.

Compound-Target-Disease Network:

In this study, this network visualizes how *Oroxylum indicum* components target psoriasis. The massive wheel at the top likely represents a dominant multi-targeted flavonoid like baicalein. This molecule directly modulates a wide

network of protein targets at once. The smaller wheel structures track complementary compounds like chrysin or apigenin. These compounds interact with overlapping subsets of the 329 therapeutic targets to create a synergistic therapeutic effect.

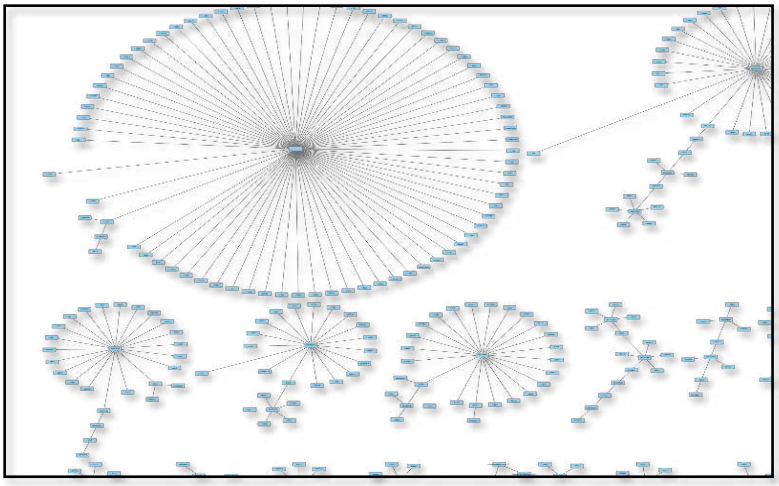

Figure 5: Compound target disease network

KEGG Pathway:

The KEGG pathway enrichment analysis revealed that the common therapeutic targets were predominantly involved in the IL-17 signaling pathway, a key regulator of psoriasis pathogenesis. The pathway was initiated through the interaction of IL-17A/IL-17F with the IL17RA/IL17RC receptor complex and IL-25 with IL17RB, leading to the activation of adaptor proteins TRAF3IP2 (Act1) and TRAF6. These signaling events subsequently activated downstream cascades involving TAK1 (MAP3K7) and the TAB1/TAB2/TAB3 complex, resulting in the stimulation of multiple inflammatory pathways, including NF-κB, MAPK, and apoptotic signaling. Activation of these pathways regulates the expression of pro-inflammatory cytokines, cellular proliferation, and apoptosis, thereby contributing to the chronic inflammatory response and epidermal hyperproliferation characteristic of psoriasis.

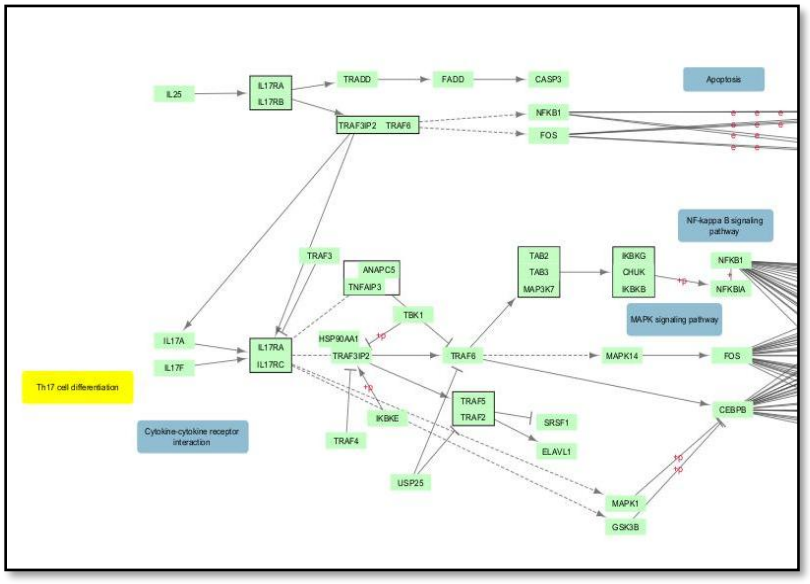

Figure 6: KEGG pathway

Integration with the Psoriasis Study

This pathway map acts as the functional blueprint connecting your entire workflow. The **329** shared targets identified in your network pharmacology analysis are the exact proteins populated across this map (like IL17A, TRAF6, and NFKB1). By using molecular docking to confirm that baicalein binds tightly to the upstream IL-17A interface, you demonstrate how the plant extract physically intercepts this cascade at the receptor level—preventing the downstream activation of the MAPK and NF-κB pathways that cause skin cell hyperproliferation in psoriasis.

String Model Protein:

Protein–protein interaction (PPI) analysis using the STRING database identified a highly interconnected network of psoriasis-associated therapeutic targets. The IL-17/IL-23 signaling axis (IL17A, IL23A, and IL23R) formed the central hub of the network and exhibited strong interactions with key inflammatory regulators, including TNF, STAT3, and TYK2, indicating their pivotal role in psoriasis pathogenesis. Additionally, proteins involved in epidermal differentiation and skin barrier function, such as LCE3B and LCE3C, were also connected within the network, suggesting a close association between immune dysregulation and impaired epidermal integrity. These findings support the involvement of multiple inflammatory signaling pathways in the therapeutic mechanism of *Oroxylum indicum*. This comprehensive in-silico screening evaluates the therapeutic potential of *Oroxylum indicum* (OI) active compounds against the immunopathological landscape of psoriasis. A network-level analysis identified 329 shared therapeutic targets situated at the critical intersection between the plant's bioactive compounds and the psoriasis disease interactome. These overlapping targets primarily map to highly interconnected hubs within the STRING database network, specifically orchestrating the IL-17/IL-23 cytokine signaling axis, TNF-alpha pathways, and intracellular TYK2/STAT3 cascades, which are responsible for driving systemic inflammation and epidermal keratinocyte hyperproliferation.

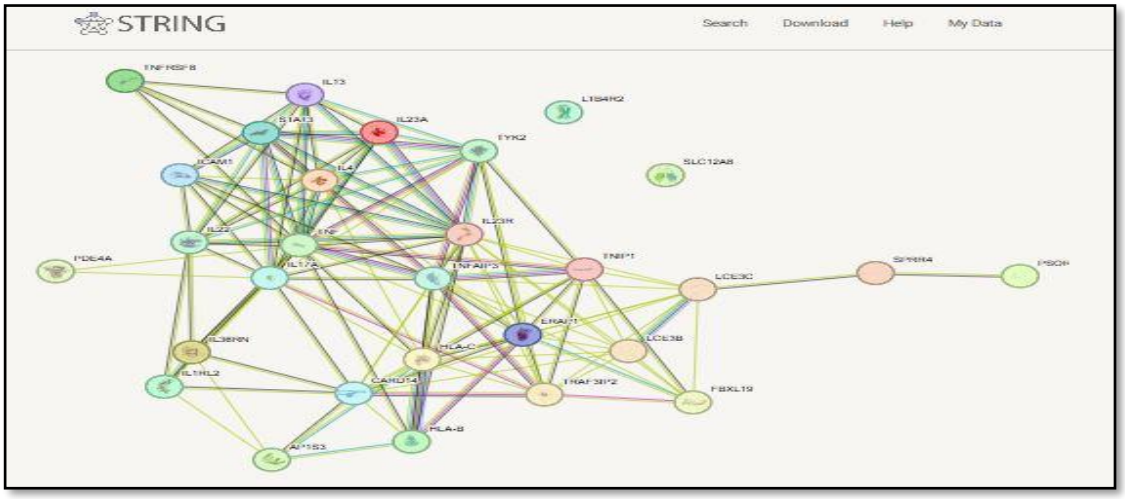

Figure 7: String model protein

Boiled Egg Model:

The SwissADME BOILED-Egg model was employed to evaluate the pharmacokinetic properties of the selected phytoconstituents. Most of the bioactive flavonoids were positioned within the high human intestinal absorption (HIA) region, indicating favorable oral absorption characteristics. These compounds also exhibited suitable lipophilicity (WLOGP 1–3) and relatively low topological polar surface area (TPSA <100 Å²), suggesting favorable physicochemical properties for oral bioavailability. Furthermore, several flavonoids, including baicalein, chrysin, and apigenin**,** were predicted to be non-substrates of P-glycoprotein**,** indicating a lower likelihood of P-gp-mediated efflux and potentially improved intracellular retention. These findings support the suitability of the selected phytoconstituents for further evaluation through molecular docking studies.

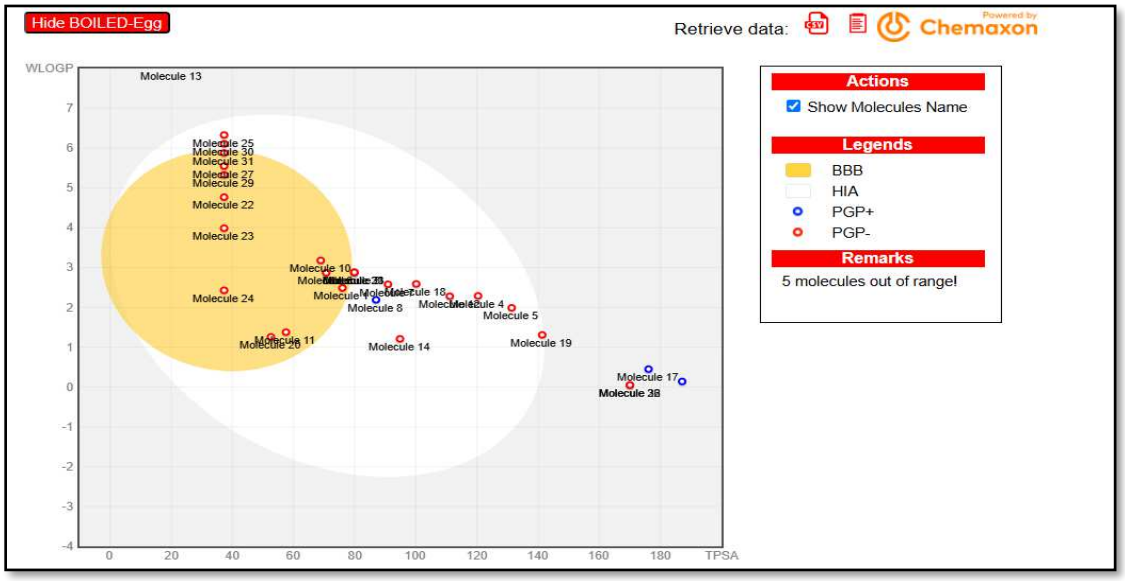

Figure 8: Boiled egg model

Molecular Docking and Structural Analysis:

The small-molecule ligand under evaluation across this entire study is Baicalein, a key bioactive trihydroxyflavone compound natively isolated from the plant *Oroxylum indicum*.

Ligand Profile

Baicalein (5,6,7-trihydroxyflavone), a major flavonoid identified in *Oroxylum indicum*, possesses a chromone backbone with three hydroxyl groups and one carbonyl group that facilitate hydrogen-bond formation with the target protein. Molecular docking analysis demonstrated a favorable binding orientation of baicalein within the active site of the IL-17A receptor, where it formed multiple hydrogen-bonding and hydrophobic interactions with key amino acid residues. These interactions suggest a strong binding affinity and indicate that baicalein may modulate IL-17A-mediated inflammatory signaling involved in psoriasis.

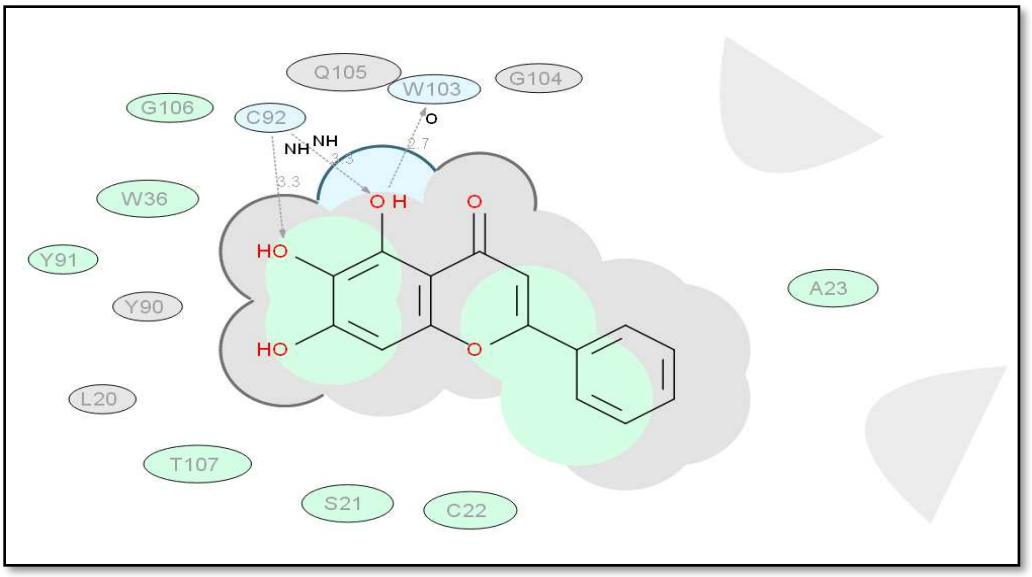

Figure 9: The 2D ligand-protein interaction profile between the bioactive flavonoid baicalein and the anti-IL-17A antibody netakimab domain (6RBB).

It captures the crucial binding variables needed to explain the molecular efficacy of *Oroxylum indicum* in treating psoriasis. Baicalein exhibited a favorable binding conformation within the active site of the target protein through multiple hydrogen-bonding and hydrophobic interactions. Hydrogen bonds were formed with Cys92 (3.3 Å) and Trp103 (2.7 Å), contributing to the stability of the ligand–protein complex. Additionally, hydrophobic interactions with Trp36, Tyr91, and Ala23 further stabilized the chromone and phenyl rings of baicalein within the binding pocket. The surrounding amino acid residues, including Gln105, Gly104, and Thr107, provided additional steric support that facilitated stable ligand accommodation, suggesting a favorable binding affinity toward the target protein.

6rbb With Baicalein

The MolSoft ICM-Pro workspace displays the molecular docking simulation of baicalein within the protein pocket. The software maps precise interactions with residues like Asp99 and Asp56 to calculate final binding scores.

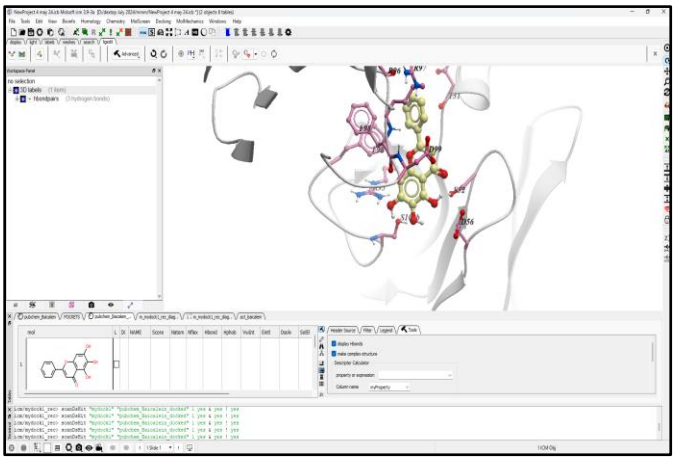

Figure 10: CRYSTAL STRUCTURE OF the VhH-domain of anti-IL-17A antibody netakimab

The MolSoft ICM-Pro interface logs a successful docking simulation for baicalein, which forms exactly three hydrogen bond pairs within the pocket.
The 3D visualization displays favourable steric complementarity anchored by critical contact residues including Asp99, Asp56, Phe88, and Ser100b.

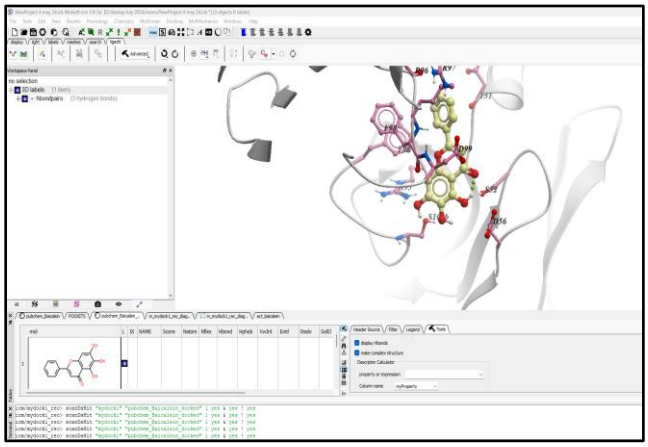

Figure 11: baicalein docked within the protein binding pocket

This 3D molecular rendering provides a detailed view of baicalein docked within the protein binding pocket, highlighting its precise orientation and intermolecular contacts.

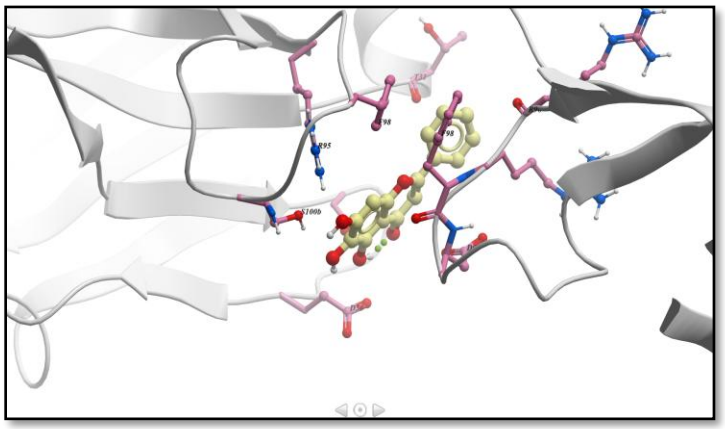

Figure 12: 3 D molecular view of baicalein

Structural Binding Insights

Molecular docking analysis demonstrated that baicalein formed a stable binding complex within the active site through an extensive hydrogen-bonding network involving its hydroxyl groups and the surrounding amino acid residues. Key residues, including Arg95, Tyr98, and Ser100b**,** contributed to the stabilization of the ligand within the binding cavity

through hydrogen-bonding and hydrophobic interactions. Furthermore, the planar chromone scaffold of baicalein exhibited a favorable orientation within the binding pocket, facilitating close interactions with the surrounding protein residues and supporting the predicted binding affinity toward the target protein.

The below figure presents the numerical docking scores and thermodynamic parameters for three distinct conformational poses of the ligand Baicalein (ID: v5281605) docked into the target protein pocket, generated via MolSoft ICM-Pro.

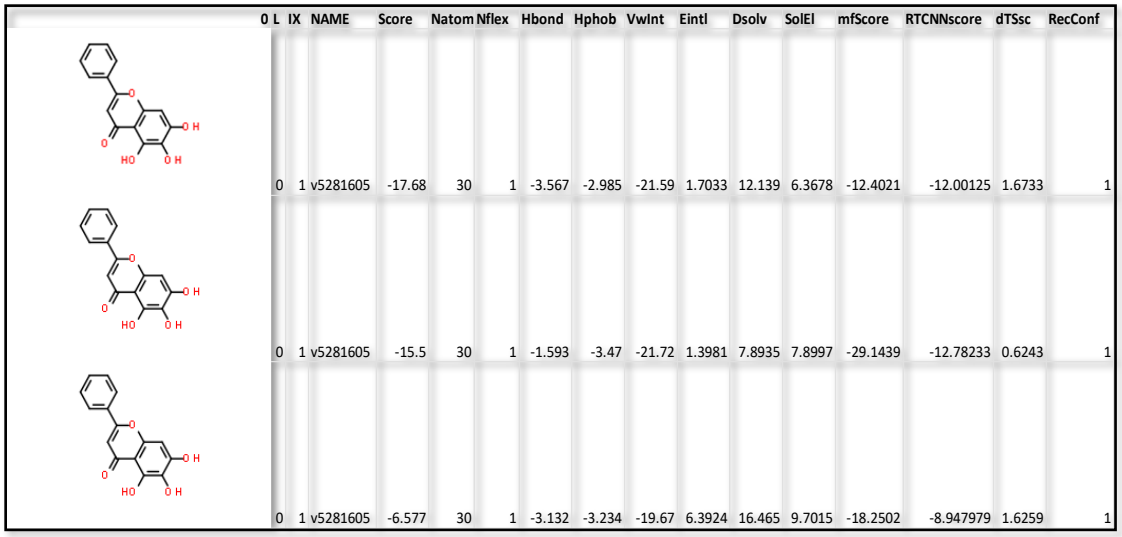

	0	L	IX	NAME	Score	Natom	Nflex	Hbond	Hphob	VwInt	Eintl	Dsolv	SolEl	mfScore	RTCNNscore	dTSsc	RecConf
	0		1	v5281605	-17.68	30	1	-3.567	-2.985	-21.59	1.7033	12.139	6.3678	-12.4021	-12.00125	1.6733	1
	0		1	v5281605	-15.5	30	1	-1.593	-3.47	-21.72	1.3981	7.8935	7.8997	-29.1439	-12.78233	0.6243	1
	0		1	v5281605	-6.577	30	1	-3.132	-3.234	-19.67	6.3924	16.465	9.7015	-18.2502	-8.947979	1.6259	1

Figure 13: Numerical docking scores and thermodynamic parameters

Conformation Comparison & Analysis

- **Pose 1 (Top Row):** This is the optimal, highest-affinity binding pose with the lowest overall docking score of **-17.68**. It is stabilized by exceptional hydrogen bonding energy (Hbond = -3.567) and a very low Van der Waals interaction penalty (VwInt = -21.59).
- **Pose 2 (Middle Row):** A strong alternative pose with a docking score of **-15.5**. While it maximizes hydrophobic grid forces (Hphob = -3.47), its hydrogen bonding configuration is weaker (Hbond = -1.593) compared to Pose 1.
- **Pose 3 (Bottom Row):** The least favourable conformation with a high docking score of **-6.577**. This pose suffers from a severe internal energy strain penalty (Eintl = 6.3924), meaning the molecule had to twist into an unstable shape to fit into this position.

Molecular docking validates these findings by confirming that baicalein, the primary flavonoid in *Oroxylum indicum*, directly targets the critical psoriasis pathway (pp. 1-2). Utilizing the crystal structure of an anti-IL-17A antibody domain (PDB ID: 6RBB), simulations show baicalein nesting within the binding pocket (pp. 1-2). The 2D and 3D models demonstrate that the compound establishes high spatial complementarity, stabilized by specific hydrogen bonds and hydrophobic interactions with key residues Cys92, Gln105, Trp103, and Gly104 (pp. 1-2). This targeted binding structurally blocks the IL-17A cytokine signalling, confirming that the highly skin-permeable components of *Oroxylum indicum* possess the exact molecular affinity required to halt plaque formation at the dermal level. When

synthesized with the SwissADME pharmacokinetic profiles, these structural insights confirm that baicalein possesses both the optimal transdermal permeability required to traverse hyperkeratotic skin barriers and the specific binding affinity necessary to neutralize downstream IL-17A cytokine signalling, providing a concrete molecular basis for using *Oroxylum indicum* in targeted topical psoriasis therapies.

Conclusion:

The present study demonstrated that the ethanolic root extract of *Oroxylum indicum* is a rich source of bioactive phytoconstituents, including alkaloids, flavonoids, glycosides, tannins, phenolic compounds, saponins, steroids, and phytosterols. Quantitative phytochemical analysis further confirmed the presence of appreciable levels of total phenolics and total flavonoids, supporting the phytochemical richness of the extract. Computational pharmacokinetic evaluation using SwissADME indicated that several flavonoid constituents possessed favorable drug-likeness and oral bioavailability profiles. Target prediction and network pharmacology analyses identified multiple psoriasis-associated therapeutic targets, highlighting the involvement of key inflammatory signaling pathways, particularly the IL-17, TNF, and MAPK pathways. Protein–protein interaction and KEGG pathway analyses further demonstrated the central role of these signaling networks in psoriasis pathogenesis. Among the identified phytoconstituents, baicalein exhibited the most favorable molecular docking profile, forming stable interactions with key amino acid residues within the target protein, suggesting its potential to modulate IL-17-mediated inflammatory signaling. Collectively, these findings provide a scientific basis for the traditional medicinal use of *Oroxylum indicum* and identify its flavonoid constituents as promising candidates for further investigation against psoriasis. Nevertheless, additional in vitro**,** in vivo**,** and clinical studies are required to validate the computational predictions and establish their therapeutic efficacy.

Consent for publication: All authors are agreeing to publish the article in this journal

Data Availability Statement: The datasets generated during and/or analyzed during the current study are available from the corresponding author on reasonable request

Availability of data and materials: The datasets generated during and/or analyzed during the current study are available from the corresponding author on reasonable request.

Competing Interests: The authors declare that they have no known competing financial interests or personal relationships that could have appeared to influence the work reported in this paper.

Funding: The present research work is not financially supported by any funding agency.

Authors' contributions:

Manisha Murgude: **Experimental work, data generation, manuscript drafting and editing**

Sandip Patil: **Supervision, guidance**

Conflict of interest: Authors so not report any conflict of interest with this manuscript

Funding statement: This work is not financially supported by any funding agency

Ethical declaration: Not applicable

References

1. World Health Organization. Global report on psoriasis [Internet]. Geneva: World Health Organization; 2016 [cited 2026 Jun 29]. Available from: who.int.
2. Lowes MA, Suarez-Farinas M, Krueger JG. Immunology of psoriasis. *Annu Rev Immunol.* 2014;32:227-55.
3. Boehncke WH, Schön MP. Psoriasis. *Lancet.* 2015;386(9997):983-94.
4. Griffiths CE, Barker JN. Pathogenesis and clinical features of psoriasis. *Lancet.* 2007;370(9583):263-71.
5. Kamiya K, Kishimoto M, Sugai J, Komine M, Ohtsuki M. Risk factors for the development of psoriasis. *Int J Mol Sci.* 2019;20(18):4347.
6. Ray-Jones H, Eyre S, Barton A, Warren RB. One size does not fit all: the genetic landscape of psoriasis and psoriatic arthritis. *J Invest Dermatol.* 2021;141(10):2343-52.
7. Balak DM, Hajdarbegovic E. Drug-induced psoriasis: clinical presentation, pathogenesis, and management. *Psoriasis (Auckl).* 2017;7:19-32.
8. Armstrong AW, Read C. Pathophysiology, Clinical Presentation, and Treatment of Psoriasis: A Review. *JAMA.* 2020;323(19):1945-1960.
9. Rajaram R, Senthil Kumar P. Biogenic synthesis of silver nanoparticles using Oroxylum indicum root extract and their incorporation into nanohydrogels for topical antipsoriatic and antimicrobial applications. *J Drug Deliv Sci Technol.* 2022;74:103512.
10. Dinda B, SilSarma I, Dinda M, Rudrapaul P. Oroxylum indicum (L.) Kurz: An update on its phytochemistry and pharmacology. *J Ethnopharmacol.* 2015;161:185-218.
11. Tabassum N, Hamdani M. Plants used to treat skin diseases. *Pharmacogn Rev.* 2014;8(15):52-60.
12. Loizou S, Lekakis I, Chrousos GP, Moutsatsou P. Beta-sitosterol exhibits anti-inflammatory activity in human aortic endothelial cells. *Mol Nutr Food Res.* 2010;54(4):551-558.
13. Finar IL. *Organic Chemistry.* 6th ed. Vol. II. England: ELBS; 1975. p. 518.
14. Tyler VE, Brady LR, Robbers JE. *Pharmacognosy.* 8th ed. KM Varghese Company; 1981. p. 67.
15. Trease GE, Evans WC. *Text Book of Pharmacognosy.* 13th ed. England: ELBS; 1994. p. 289, 342, 388.
16. Khandelwal KR. *Practical Pharmacognosy.* 2nd ed. Pune: Nirali Prakashan; 2002. p. 149-159.
17. Khandelwal KR. *Practical Pharmacognosy Techniques and Experiments.* 10th ed. Pune: Nirali Prakashan; 2003. p. 149-154.
18. Kanehisa, M., Sato, Y., Kawashima, M., Furumichi, M., and Tanabe, M.; KEGG as a reference resource for gene and protein annotation. Nucleic Acids Res. 44, D457-D462 (2016).
19. Kanehisa, M. and Goto, S.,: KEGG: Kyoto Encyclopedia of Genes and Genomes. Nucleic Acids Res. 28, 27-30 (2000).

Supplementary Files

This is a list of supplementary files associated with this preprint. Click to download.

- tableManuscriptMurgudeInnovation02Aug2026insilicoCopyCopy.docx